Large-Format Preparation Technology and Electric Heating Performance of Wooden Electric Heating Flooring

Pu Ti,[a,b] Yonghua Liao,[a,b] Quanyu Wang,[a,b] Zhangji Qin,[c] Qingyuan Cai,[c] Zhi Lin,[a,b] and Quanping Yuan [a,b,*]

A large-format manufacturing process of electric heating floors for indoor heating was evaluated in this work using large-format high-density fiberboard as the substrate, carbon fiber paper as the electric heating element, and semi-cured melamine resin film as the bonding material to elevate its production efficiency. The semi-cured melamine resin film permeated the carbon fiber paper to form a glued structure *via* hot-pressing process, which improved the water resistance and insulation of the electric heating layer. The internal bonding strength of the floor reached 1.63 MPa with the enhanced waterproof properties. The temperature rise of both the electric heating floor and the assembled floors can reach 20.5 °C within 60 min under the voltage of 220 V. There was a small difference of approximately 2 °C in the ambient temperature between the heights of 0.6 m and 1.8 m above the running assembled electric heating floors. The power of the assembled 16 pieces of floors stabilized at 830 W after the continuous electrification for 12 h in this test condition, which demonstrated the comfortable and high-efficiency heating performance of the assembled electric heating floors.

DOI: 10.15376/biores.17.3.4069-4085

Keywords: Electric heating floor; Large-format manufacture process; Fiberboard; Semi-cured melamine resin film; Carbon fiber paper; Power consumption

*Contact information: a: School of Resources, Environment and Materials, Guangxi University, Nanning 530004, China; b: MOE Key Laboratory of New Processing Technology for Non-ferrous Metals and Materials & Guangxi Key Laboratory of Processing for Non-ferrous Metals and Featured Materials, Guangxi University, Nanning 530004, China; c: Guangxi Fenglin Wood Industry Group Co. Ltd, Nanning 530221, China; *Corresponding author: quanpingy@163.com; yuanquanping@gxu.edu.cn*

INTRODUCTION

Compared with other indoor heating methods, floor heating has attracted more and more attention due to its comfortability (Sarbu and Sebarchievici 2014). Radiant floor heating can be achieved with hot water pipe (Boahen *et al.* 2021), electric heating film (Yi *et al.* 2017), and electric heating cables, among other methods. Electric heating film has attracted more and more attention from consumers due to its advantages of easy installation, excellent thermal conversion efficiency (Wang *et al.* 2021), and electric heating performance. Related research had prepared a wooden electric heating functional board with built-in carbon fiber paper as an electric heating element (Song *et al.* 2015). Carbon fiber paper is a film-like electric heating material made of carbon fiber and plant fiber. Plant fiber acts as a skeleton for the wide lap network of carbon fiber, which gives carbon fiber paper a potential large-format electric heating element. The structure and

morphology of the carbon fiber paper did not change significantly at a temperature of 110 °C (Song *et al.* 2017). At the same time, when the power density of 500 W/m^2 was loaded, its surface temperature can be increased by 20 ℃ within 10 min, and the temperature difference was 2 °C (Yuan and Fu 2014). The work used a modified urea-formaldehyde resin adhesive *via* a roller coating to bond the carbon fiber paper and the veneer to prepare an electrothermal composite by hot-pressing process. However, the gluing uniformity of the liquid adhesive was greatly affected by the gluing method and the gluing amount, which could increase the temperature difference. The type of gluing was not conducive to shifting the electric heating film in the lay-up stage. In addition, semi-cured melamine resin film as adhesive was also employed to prepare electric heating composites, which have better power control ability with a small change rate of resistance (Yang *et al.* 2017). High-density floorboard substrates for floor heating displayed a higher heat transfer rate than that of plywood due to their density and thickness (Seo *et al.* 2011). There has been little research on high-density fiberboard substrates for electric heating flooring. The existing studies on wooden electric heating composites and flooring primarily focus on small-size wooden substrates, which leads to a low production efficiency. There is also a lack of research on the indoor application performance of electric heating flooring, as well as their electric connected method.

In this study, a large-format manufacturing process for electric heating floor with high-density fiberboard substrate, large-format carbon fiber paper as the electric heating element, and semi-cured melamine resin film as the bonding material was proposed to enhance its industrialization production. The use of the semi-cured melamine resin film was conducive to shifting the electric heating element and can reduce its fold in the lay-up stage, thus elevating the paving efficiency of the electric heating layer. At the same time, the semi-cured melamine resin film can penetrate into the carbon fiber paper to form a glued structure, which can endow the electric heating layer with enough mechanical strength and insulation properties. In addition, pre-processed holes for the wiring distributed at the bottom fiberboard of the floor are more convenient for the assembly of the floors. The wires between the electric heating floors are connected *via* insulated electric connectors. This presented process can obtain 12 pieces of full-size electric heating floors at one time, which have low differentiation of their power or resistance as well as good running stability and electric heating performance. In addition, the indoor heating performance with the floors was studied after 16 pieces of the floor were assembled indoors. This study will provide technical reference for the efficient production of wooden electric heating floors.

EXPERIMENTAL

Materials

High-density fiberboard, with length and width dimensions of 2440 mm × 1220 mm, an average thickness of 5 mm, and a density of 0.906 g/cm^3, were provided by Guangxi Fenglin Wood Industry Group Co. (Nanning, China). The carbon fiber paper had a thickness of approximately 0.1 mm and a surface sheet resistance of about 200 Ω/sq. The volumed copper foil with a thickness of 0.01 mm was purchased from Dongguan Shichengjin Co. (Dongguan, China) and cut into a width of 8 mm. The semi-cured melamine resin film with a thickness of approximately 0.1 mm was provided by the Nanning Haichuan Decorative Materials Factory (Nanning, China).

Methods

Preparation of the electric heating layer with small dimension

As shown in Fig. 1, the carbon fiber paper was cut into a small 60 mm × 80 mm piece. Adhesive tape was used to fix the copper foil on both sides of the carbon fiber paper to prevent the copper foil from sliding. The effective area between the two copper foils electrodes was 60 mm × 60 mm. The characterization of the microstructure was carried out and the electric heating performance was tested.

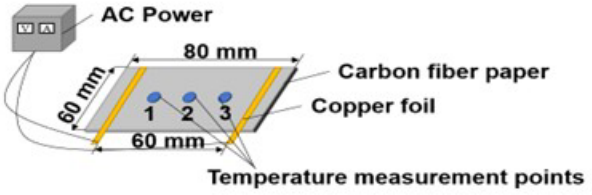

Fig. 1. Structure of the electric heating layer

Manufacturing process of the large-format electric heating floor

To begin, the structure of the large-format bottom high-density fiberboard shown in Fig. 2 was processed. The wiring hole with a diameter of 7 mm was designed at a distance of 60 mm from both ends of the board. The wiring hole in the middle position was located at the distance of 60 mm to both sides of the center line of the board.

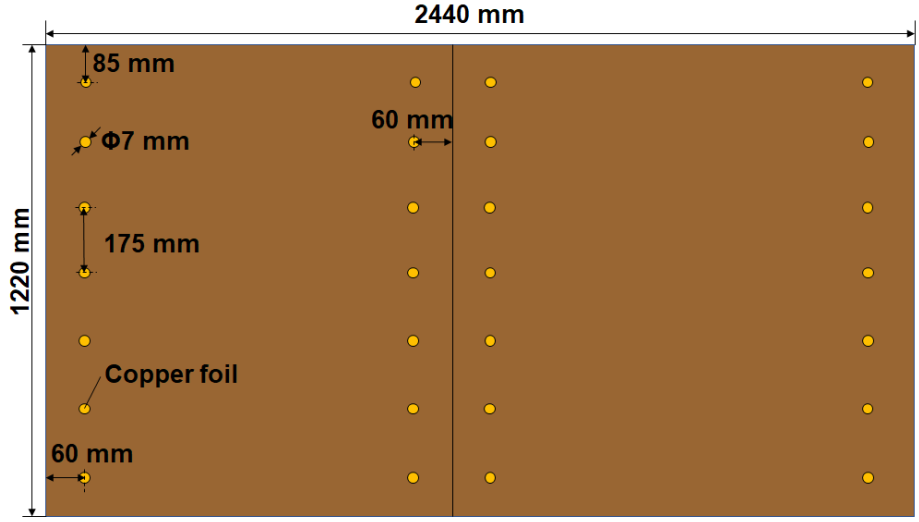

Fig. 2. The structure of the large-format bottom high-density fiberboard (loss of saw kert in the machining process had been considered in this structure design)

As shown in Fig. 3, the bottom high-density fiberboard, the semi-cured melamine resin film, the copper foil belt, the carbon fiber paper, the semi-cured melamine resin film, and the surface high-density fiberboard were layered from the bottom to the surface, respectively. Subsequently, the composite was hot-pressed to create the large-format electric heating floor substrate with an HSYJ-1600T type of double-sided pressing system (Wuxi Lutong Machinery Co., Wuxi, China) through a one-time hot-pressing process. The hot-pressing process was conducted for 5 min at a pressure of 1.3 MPa and a temperature of 130 °C. Finally, the large-format substrate was veneered with the impregnated adhesive

paper and wear-resisting layer on the surface, as well as the balance layer on the undersurface of the substrate *via* the hot-pressing process. The substrate was further machined by Guangxi Bojing Floor Co. (Nanning, China), where it was cut and mortised to obtain an electric heating floor with a length of 1210 mm and a width of 160 mm (Fig. 4). The wire was connected to the copper foil with an electric soldering iron. At the same time, the welding position was filled with hot melt adhesive to prevent current leakage. The wires among the electric heating floors were connected by insulated electric connectors. The end of the wire was fixed in the plug as the voltage input terminal of the electric heating floor.

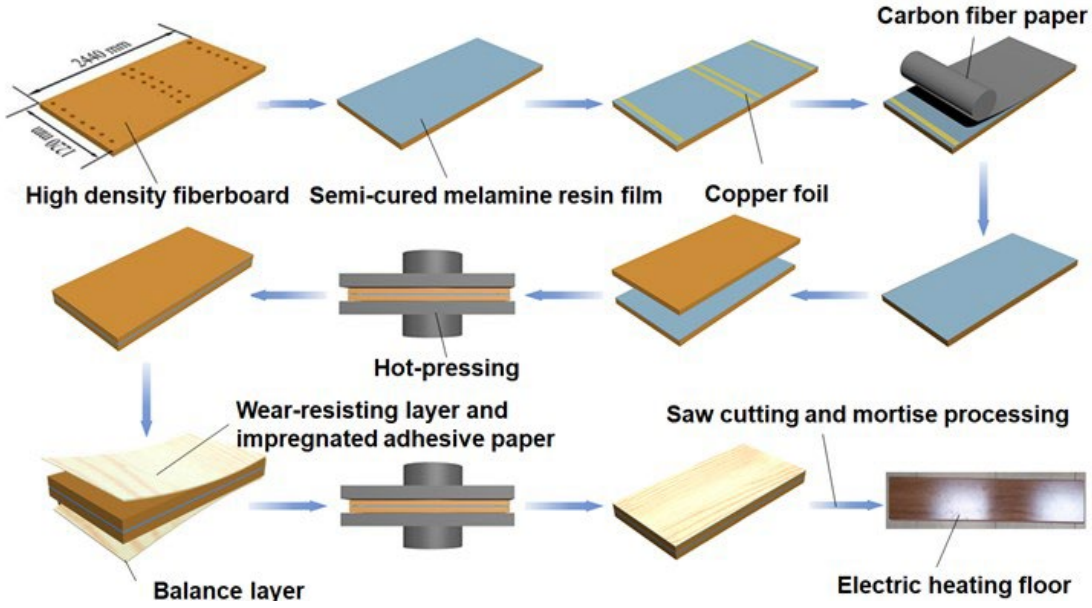

Fig. 3. The large-format preparation process of the electric heating floor

Three temperature measurement points, shown in Fig. 4a, were set at the center point of the floor surface and at points 300 mm on each side of the center point of the length. Two temperature measurement points, shown in Fig. 4b, at the floor bottom were located at distance of 200 mm on each side of the center point.

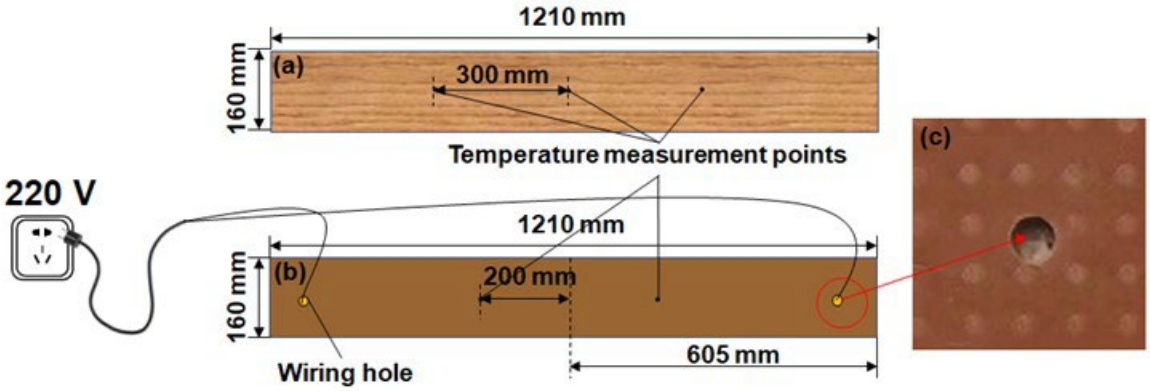

Fig. 4. The distribution of temperature measurement points a) on the board surface, b) on the bottom and c) wiring diagram of the floor

Microstructure characterization of the electric heating layer

An S-3400N scanning electron microscope (SEM, Hitachi) was used to analyze the microstructure of the carbon fiber paper and the electric heating layer in the floor after the hot-pressing process.

Electric heating performance of the electric heating layer and electric heating floor

The electric heating layer was loaded with different power densities (100, 300, 500, 700, and 900 W/m^2) for 30 min using an adjustable DC power supply and then cooled for 10 min. During the loading process, the surface temperature of the electric heating layer was recorded every second with a temperature recorder (SIN-R960; Hangzhou Sinomeasure Automation Technology Co., Zhejiang, China).

After the thin sheet thermocouple was attached on the temperature measurement points, as shown in Fig. 4, the electric heating floor was electrified with 220 V for 12 h. The temperature data was recorded every second using the temperature recorder to analyze the temperature rise law of the electric heating floor within 12 h.

The electric heating floor was loaded with different power densities (100, 150, 200, 250, 300, and 350 W/m^2) for 2 h to explore the relationship between the power density and the temperature rise. The effective heating area of the electric heating floor was 1100 mm × 160 mm, which was used for the calculation of the applied voltage. The various voltages were gained *via* regulation using the adjustable AC power supply (STG-3000W, regulating range of 0-300V, Shanghai Delixi Switch Co., Ltd., Shanghai, China).

In addition, the stability of resistance between two electrodes in the electrified process was evaluated. As shown in Fig. 4b, the 220 V was directly used for continuous power on the electric heating floor for 12 h. A Fluke 15B+ digital multimeter was used to measure the resistance between the two electrodes every hour in the short-time power off condition. The resistance stability in the cyclic electrification was also tested to analyze its running stability. The electric heating floor was subjected to a cycle electrifying test of power-on for 1 min and power-off for 30 s under the voltage of 220 V. The digital multimeter was used to record the resistance of the electric heating floor after every 10 cycles of the total 180 cycles.

Analyzation of the indoor heating performance of the assembled electric heating floors

Sixteen pieces of the electric heating floors (approximately 3 m^2) were jointed *via* their mortise in a room with a temperature of about 29.5 ℃ and a relative humidity of 44%RH. The floors were paved above the 6 mm thick heat-insulating film and the keels (Fig. 5a). The electric connection to every floor was implemented in parallel circuits.

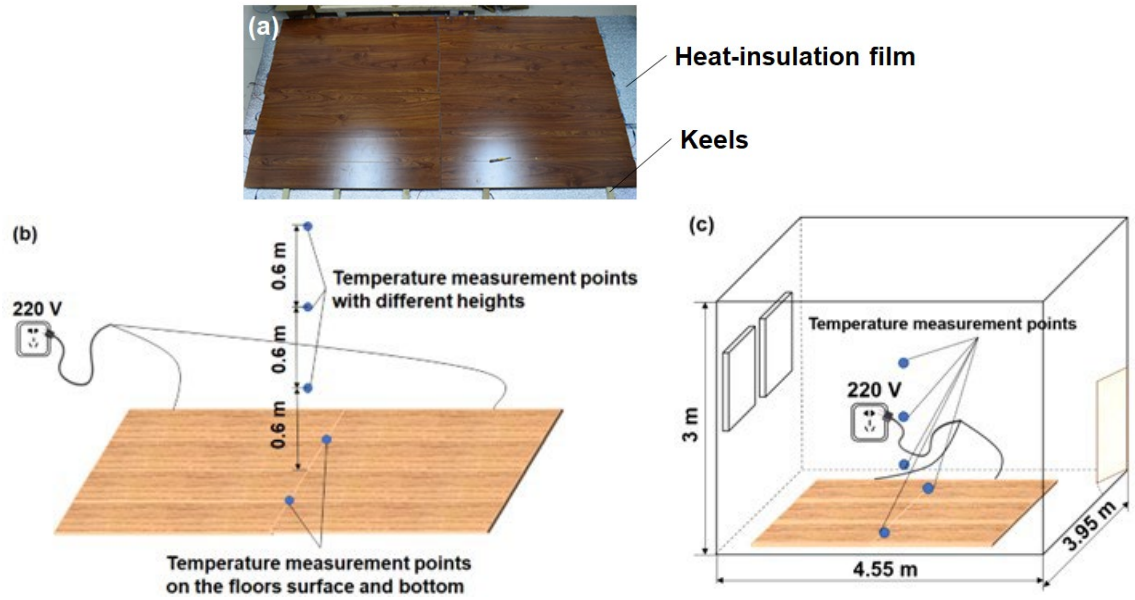

Fig. 5. The a) assembly of the electric heating floors indoors and the b, c) distribution of the temperature test points at different heights

The ambient temperature at different heights in the indoor space (Figs. 5b and c) was measured to preliminarily evaluate the practical heating performance, as well as the two test points on the floors surface and bottom. The thermocouple connected to the temperature recorder was set up at the test points.

The assembled electric heating floors were energized using the power supply of 220 V for 12 h. All the temperature data at various temperature measurement points were recorded to analyze the actual electric heating performance. In addition, the electric power and power consumption of the floors was monitored *via* an AC digital display multi-function meter (PZEM-061, Shenzhen Shengke Electronics Co., Shenzhen, China). During the power-on process, the temperature distribution on the floors was evaluated every hour with the help of a Fluke TiS40 infrared thermal imaging camera to analyze its temperature uniformity.

Physical and mechanical performance of the electric heating floor

The surface bonding strength, the internal bonding strength, the modulus of rupture, and the thickness-swelling rate of water absorbing of the electric heating floor was tested according to the Chinese standard of GB/T 18102 “Laminate floor coverings” (2020).

RESULTS AND DISCUSSION

Micro-morphology of the Electric Heating Layer

As shown in Fig. 6a, the carbon fibers and the plant fibers were arranged in a disorderly manner with an overlapping network structure in the carbon fiber paper that was conducive to the penetration of the adhesive.

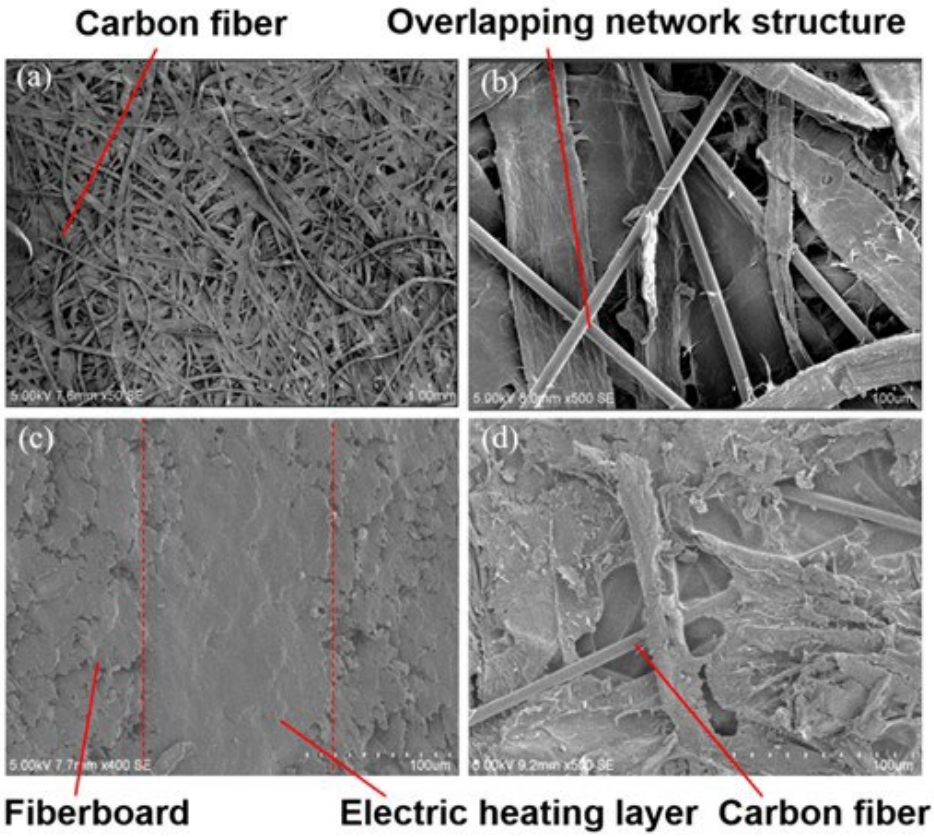

Fig. 6. The a, b) surface SEM analysis of the carbon fiber paper, the c) cross section morphology of the electric heating layer after hot pressing, and the d) teared surface of the electric heating layer after hot pressing

There was a lap structure among the carbon fibers in the carbon fiber paper, shown in Fig. 6b, by which a conductive path can be formed to endow with conductivity and the electric heating performance (Gong *et al.* 2016). From the morphology of cross section of the floor (Fig. 6c), the electric heating layer was compactly bonded to the high-density fiberboard without an obvious gap. This fact indicated that the application of semi-cured melamine resin film can provide good bonding strength *via* the presented large-format manufacturing process. The carbon fiber observed in Fig. 6d showed no obvious morphological change after hot pressing, which indicated that it could maintain good thermal stability at a certain temperature (Song *et al.* 2017) when the floor runs in normal conditions. The semi-cured melamine resin infiltrated in the carbon fiber paper to form a stable glued structure, by which the overlapping structure among the carbon fibers was strengthened and the number of the overlap in conductive network was increased. This enhanced the conductivity and the electric heating performance of the electric heating layer.

Electric Heating Performance of the Electric Heating Layer and Electric Heating Floor

As shown in Fig. 7, the stable surface peak temperature on carbon fiber paper was positively correlated with the power density. This finding was similar to reported results (Zhao *et al.* 2011; Song *et al.* 2017). The temperature and its rising velocity of the electric heating layer can be regulated by controlling the input power (Yuan and Fu 2014).

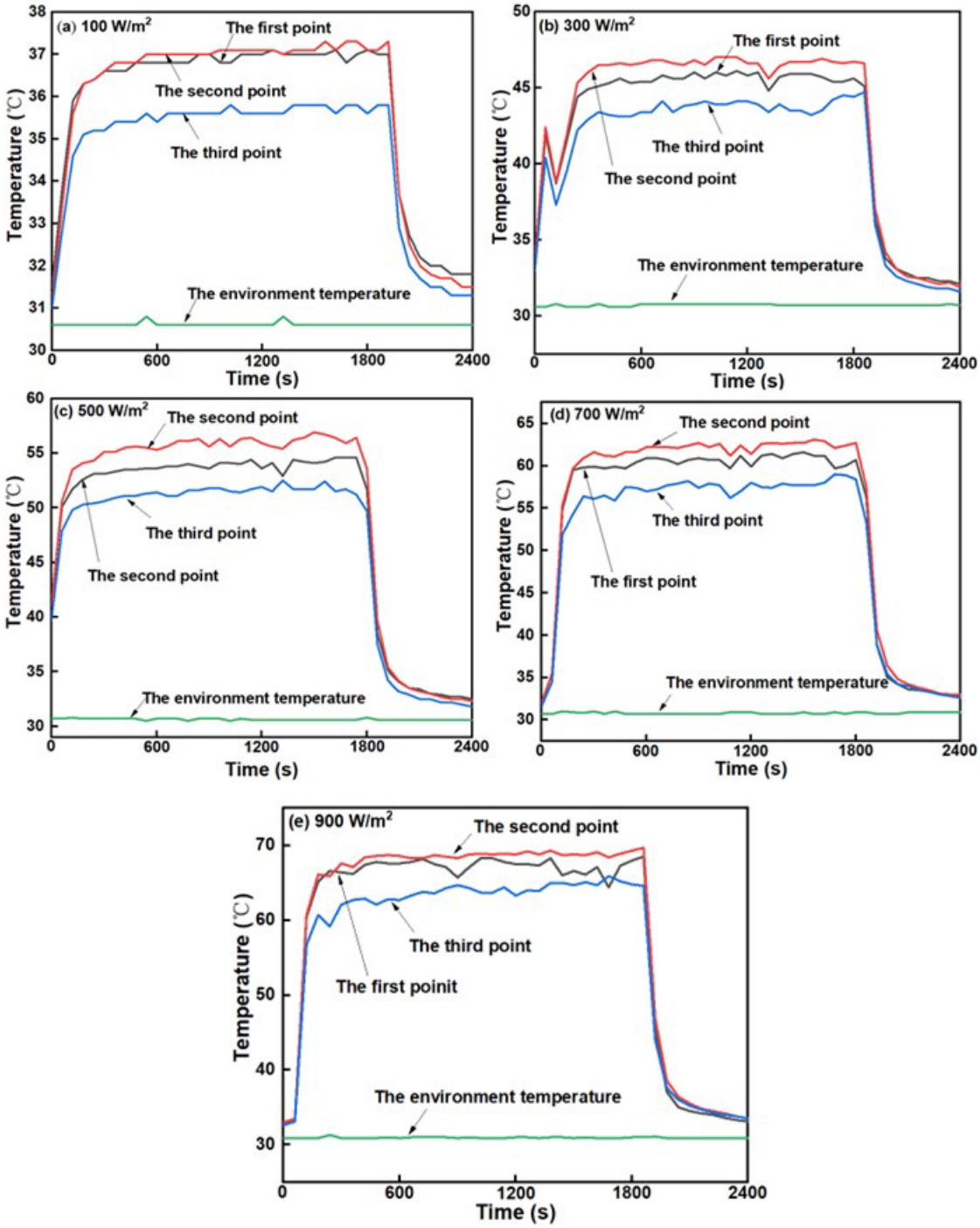

Fig. 7. The temperature rising trend of the carbon fiber paper loaded with power densities of a) 100 W/m^2, b) 300 W/m^2, c) 500 W/m^2, d) 700 W/m^2, and e) 900 W/m^2

Carbon fiber has good thermal stability (Pradere *et al.* 2009), electric heating response speed, and heat transfer efficiency, which will contribute to enhancing the electric heating performance of its composite. The temperature rise ranged from 4.8 to 36.7 °C as the power density ascended from 100 to 900 W/m^2. The electric heating layer can run at an average rising rate of approximately 1.5 °C/min in the rapid heating stage under the various powers. There is also thermal conduction and radiation conduction for the large specific

surface area of carbon fiber. It can be seen that electric heating performance of the electric heating floor is suitable for the indoor heating in winter when the outdoor environment temperature is about 0 to 5 °C or even the lower temperature.

As shown in Fig. 8, the surface temperature rise of a single piece of electric heating floor can reach 20.5 °C, while the bottom temperature rise can reach a slightly higher temperature rise of approximately 24.8 °C. The surface temperature rise of electric heating floor reached about 20.5 °C under voltage of 220V (about 296 W/m^2), which was about 3.0 °C higher than that of electric heating plywood under 300 W/m^2 (Yang *et al.* 2017). The average temperature difference between the surface and the bottom of the electric heating floor was 4.6 ℃, which was lower than that of the carbon fiber paper electric heating plywood (6 ℃) at the power density of 300 W/m^2 (Yang *et al.* 2017). Meanwhile, the surface temperature rise of the electric heating floor reached 20 °C after it had been energized for 1 h. Heat storage phenomenon generated in the narrow space between the bottom of floor and heat-insulating film. Therefore, the bottom temperature of the floor was higher.

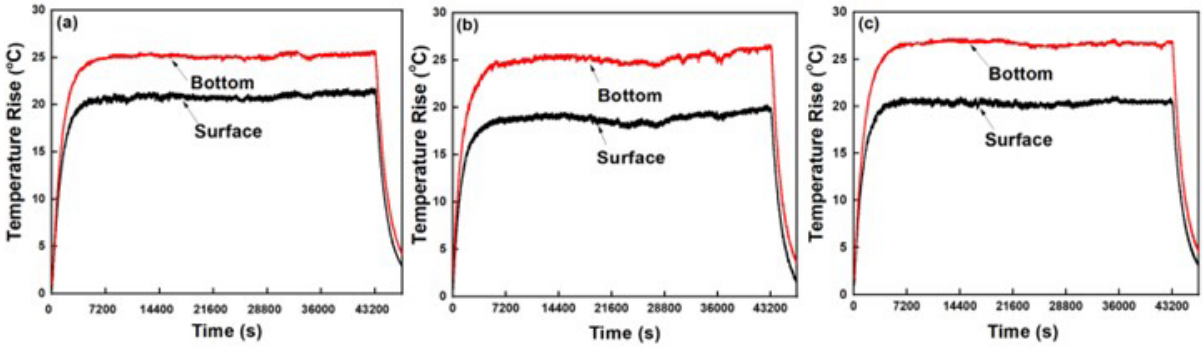

Fig. 8. The temperature rising trend of the electric heating floor directly connected to the 220 V supply for the a) first sample, b) second sample, and c) third sample

The surface temperature difference will directly affect the user with the use of floor heating. As shown in Figs. 9a, 9b, and 9c, the temperature difference on the center area in the whole electric heating floor was approximately 5.5 °C, 4.2 °C, and 4.3 °C for the three repeated floors, respectively. As for the high heat transfer and homogeneity of high-density fiberboard, the temperature difference of electric heating floor was lower than that of the electric heating plywood (Yang *et al.* 2017). Moreover, the temperature difference in the smaller area on the electric heating floor was as low as approximately 3.0 °C, 3.0 °C, and 2.3 °C (Figs. 9d, 9e, and 9f), respectively, which indicated the process stability of the electric heating floor even with the large-format process.

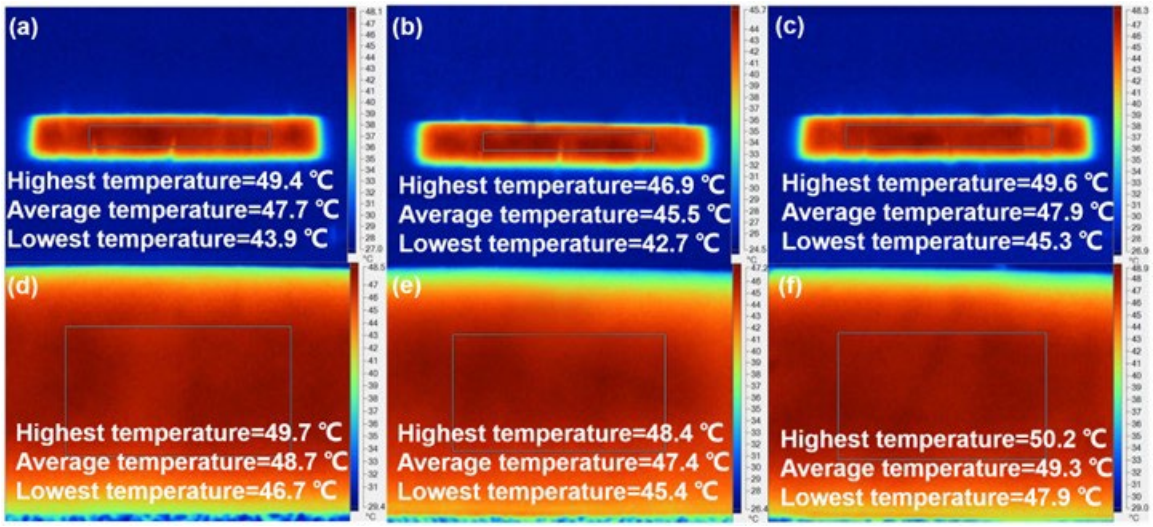

Fig. 9. The a, b, c) infrared thermal image of three pieces of electric heating floors directly connected to the 220 V supply after being electrified for 6 h; the d, e, f) infrared thermal image of the smaller area on the electric heating floor

As can be seen in Fig. 10, the temperature on the electric heating floor reached the stabled state after the electrification for approximately 1 h under different power densities.

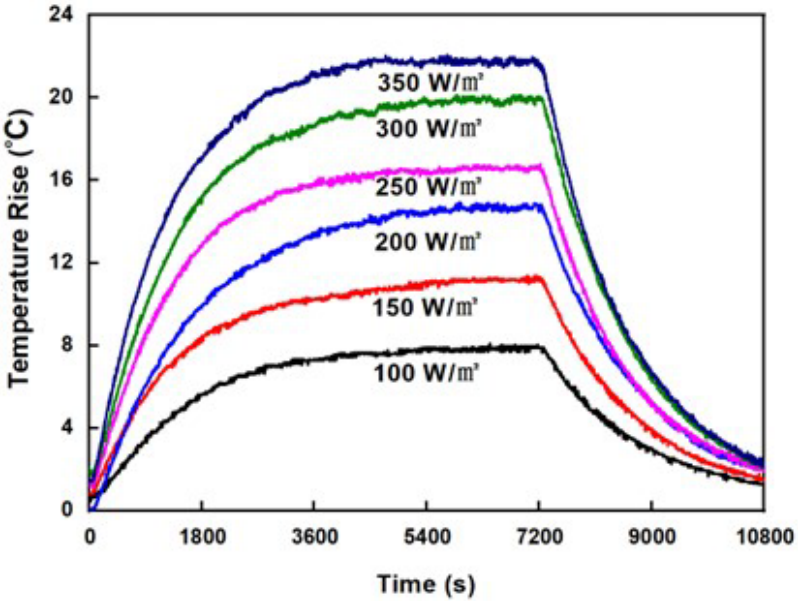

Fig. 10. The relationship between the time and temperature rise of the electric heating floor under various power densities

When the power density was increased by 50 W/m^2, the highest temperature of the electric heating floor climbed by approximately 2 °C, which showed a good linear relationship. The surface temperature rise curve was consistent with that of the electric heating layer above. Therefore, the temperature control of the electric heating floor can also be realized easily and accurately by adjusting the power density.

The resistance of the electric heating floor decreased sharply and then slowly with the extension of the initial power-on time (Fig. 11a) when the temperature climbed

gradually and achieved the equilibrium state. This can be seen as negative temperature coefficient effect (NTC) in this process. The increase of the conductive path among the carbon fibers reduced the resistance because of electricity and heat (Di *et al.* 2003). The drop rate of the resistance (DRR) of the electric heating floor was as low as approximately 1.2% after the power-on test, which indicated that the electric heating floor had good power stability.

In addition, power on/off times had a similar effect on the resistance, as can be seen in Fig. 11b. The resistance stabilized after approximately 100 cycles in this test condition, and the DRR was approximately 0.9%. Compared with the 1.25% DRR of the electric heating plywood (Yang *et al.* 2017), the floors exhibited better power stability.

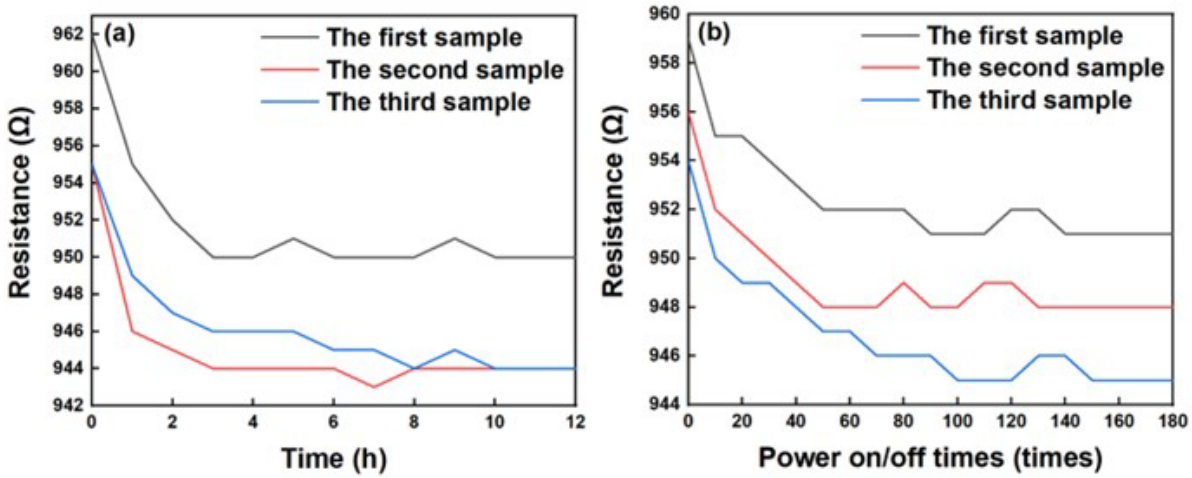

Fig. 11. The relationship between the a) time and resistance of the electric heating floor and the b) power on/off cycles and the resistance

Indoor Simulation Performance of the Assembled Electric Heating Floors

The electric heating floors were assembled in an indoor environment with the closed door and window without air convection equipment. After the assembled electric heating floors were electrified by connecting to a 220 V supply source, the ambient temperature (located at a height of 0.6 m outside the floors) climbed primarily in the 6 h ahead when the surface temperature of the floors rose faster at this stage (Figs.12a and 12b). Finally, the ambient temperature was maintained at approximately 35.2 °C in this measurement condition.

The surface temperature rise of the floors (Fig. 12b) was approximately 23.8 °C and the bottom temperature rise was about 29.3 °C in the stable state. The main temperature rise period on the surface of the electric heating floor was concentrated in the previous 1 h. At the same time, compared with a single electric heating floor shown in Fig. 8, the assembled electric heating floors had a slightly higher stabilized temperature.

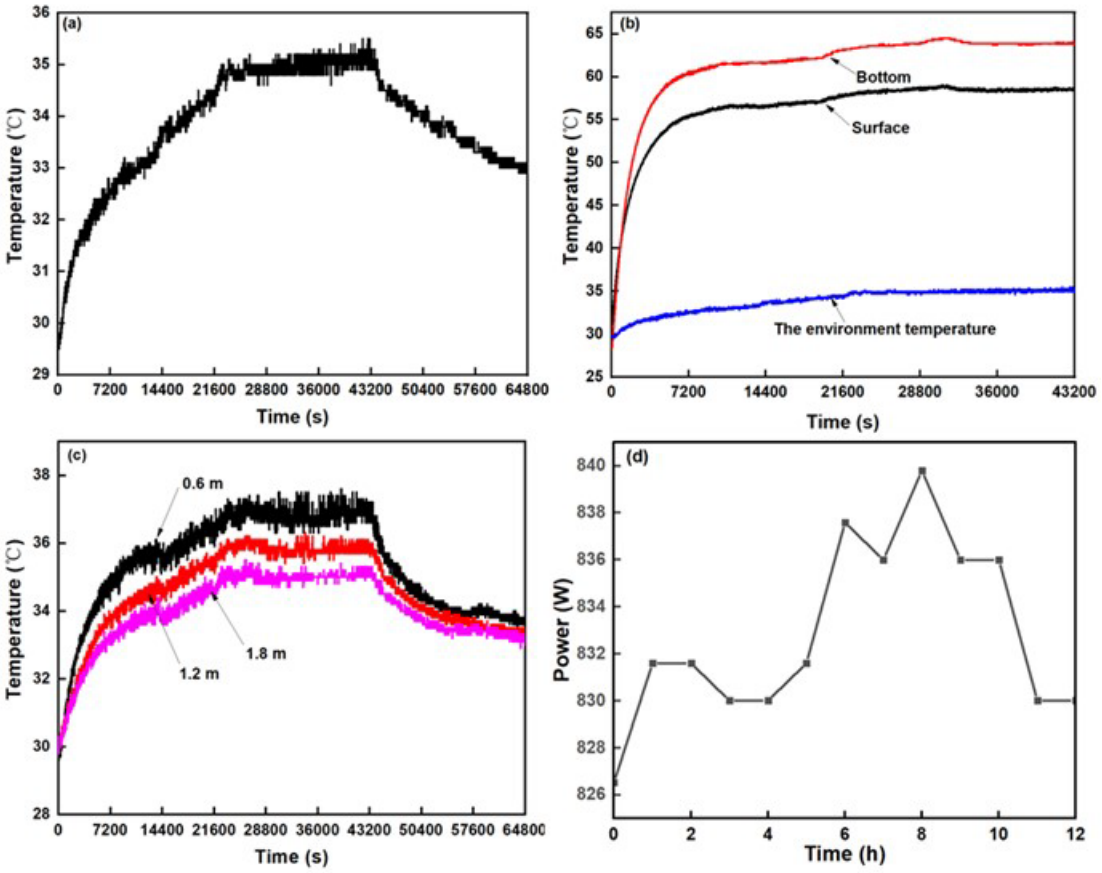

Fig. 12. The a) relationship between the time and ambient temperature (the temperature measurement point was located at height of 0.6 m outside the assembled electric heating floors), b) relationship between the time and temperature on the surface and bottom of the floors in the temperature rise stage, c) relationship between the time and ambient temperature at different heights above the floors, and d) actual running power of the floors monitored *via* the AC digital display multi-function meter

As can be seen in Fig. 12c, the ambient temperature at different heights above the floors exhibited a gradient distribution. The temperature difference between the height of 0.6 and 1.8 m was approximately 2 °C. As shown in Fig. 12d, the power of the floors stabilized at about 830 W after 12 h under the 220 V. The fluctuant rise in the continuous energization was attributed to the slow drop of the resistance, which was found from the single electric heating floor.

As shown in Table 1, the power consumption had a good linear relationship with time. After running for 12 h, 10.01 KW·H of electrical energy was consumed by the floors and the average hourly energy consumption was calculated as about 0.83 KW·H.

Table 1. Power Consumption of the Assembled Electric Heating Floors in the Running of 12 h

Time (h)	1	2	4	6	8	10	12
Power consumption (KW·H)	0.84	1.68	3.31	4.97	7.57	8.41	10.01

The power stability of the assembled electric heating floors can also be checked by calculating the power density of single electric heating floor. The power density of the single electric heating floor can be calculated by Eqs. 1 and 2,

$$P_{(Actual\ power)} = \frac{U^2}{R} \quad (1)$$

where $P_{(Actual\ power)}$ is the power during the electrification process of the electric heating floor (W), U is the input voltage when the electric heating floor is energized (V), and R is the stable resistance after the electric heating floor is energized (Ω).

$$P_{(Actual\ power)} = P_{(Power\ density)} \times S_{(Area)} \quad (2)$$

In Eq. 2, $P_{(Actual\ power)}$ is the power during the electrification process of the electric heating floor (W), $S_{(Area)}$ is the surface area of the electric heating floor (m^2), and $P_{(Power\ density)}$ is the power per square meter of the electric heating floor (W/m^2).

As shown in Eqs. 1 and 2, the surface area of the electric heating floor has a certain influence on the power density when the running power is stable. The effective area between the two electrodes of an single electric heating floor was 1100 mm × 160 mm, so its power density was 296 W/m^2. By the calculation, the power of the assembled electric heating floors is about 834 W (296 W/m^2×1.1 m×0.16 m×16). The calculated results were in good agreement with the actual test results (about 830 W), which also indicated the good power stability of the assembled electric heating floors. However, the actual surface area of the whole electric heating floor was 1210 mm× 160 mm. Therefore, the actual power density was 269 W/m^2.

As seen from the surface infrared thermal image in Fig. 13, the surface peak temperature of the floors was maintained at approximately 55 °C after the continuous energization for 3 h. The surface temperature difference of each electric heating floor observed by infrared thermal imager was small, and there was a stable running performance with no abnormal local high temperature phenomenon. There was a high production efficiency of the electric heating floor prepared by the large-format process and there was a small performance difference among the various floors, without a large temperature drop at the seam between two floors. At the same time, due to the higher efficiency of heat exchange between the edge area of the floors and the environment, the temperature in the edge area was lower than the temperature in the center area.

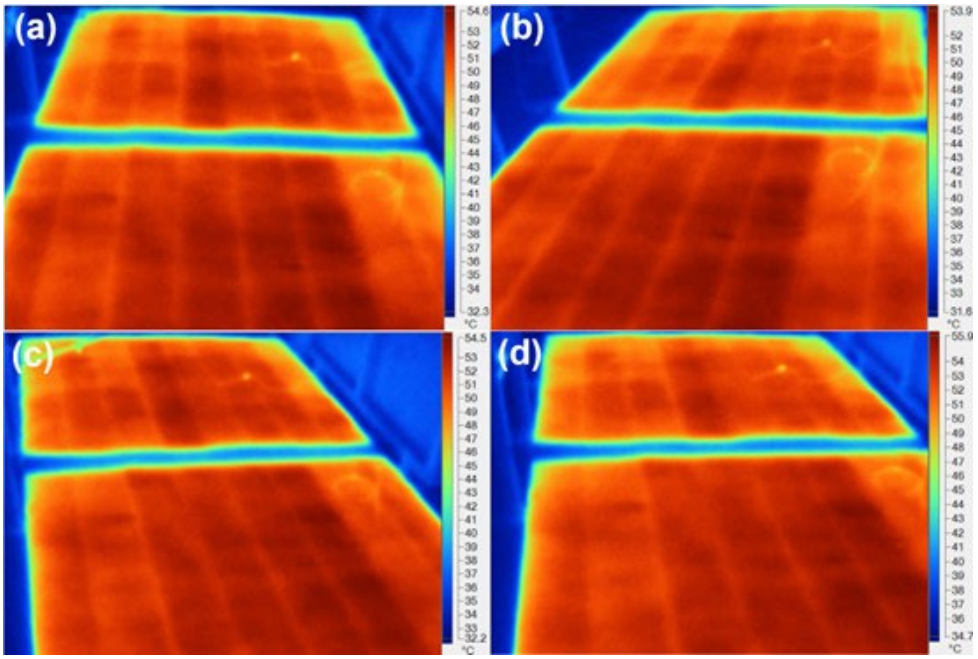

Fig. 13. The infrared thermal image of the assembled electric heating floors power on after a) 3 h, b) 6 h, c) 9 h, and d) 12 h

An exponential curve relationship can be found between heating time and temperature rise *via* data fitting (Eq. 3 for the surface and Eq. 4 for the bottom), as shown in Fig. 14). The surface temperature rise of the floors could reach about 25 °C after 105 min. The space at the bottom of the assembled electric heating floors was relatively closed, resulting in higher temperature than that on the surface in the running process.

$$y=26.10-25.82e^{-x/2227.55} \ (R^2=0.995) \quad (3)$$

$$y=34.23-34.55e^{-x/2002.00} \ (R^2=0.997) \quad (4)$$

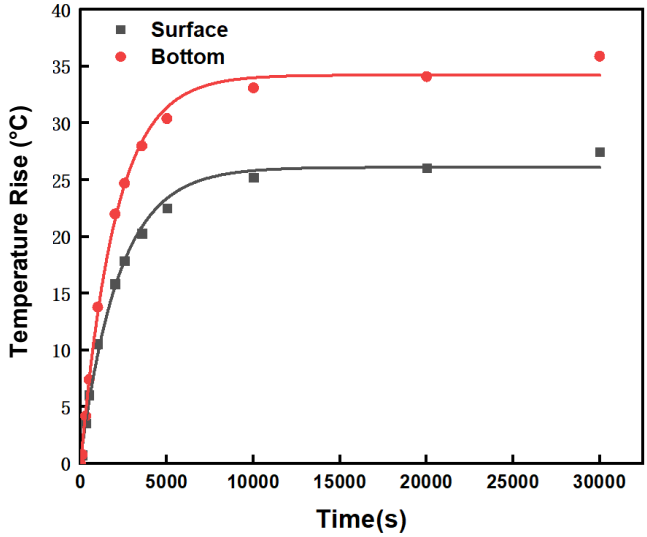

Fig. 14. Time-temperature rise relationship of the assembled electric heating floors

Physical and Mechanical Properties of the Electric Heating Floor

The physical and mechanical properties of the electric heating floor shown in Table 2 conform to the requirements of GB/T 18102 standard (2020). The specimens after the test in Fig. 15a showed that there was good bonding performance between the electric heating floor substrate and the impregnated adhesive paper. As shown in Fig. 15b-e, the fracture site during the test on modulus of rupture and internal bonding strength was located at the high-density fiberboard rather than at the electric heating layer, indicating the high bonding strength between the electric heating layer and the fiberboard with the use of semi-cured melamine resin film. In addition, there was no visible destruction in the electric heating layer after the measurement of the thickness swelling rate of water absorption (Figs. 15f and 15g). Consequently, these results indicate that the use of semi-cured melamine resin film enhances waterproof and bonding strength of the electric heating layer in the floor.

Table 2. Physical and Mechanical Properties of the Electric Heating Floor

Surface Bonding Strength (MPa)	Internal Bonding Strength (MPa)	Modulus of Rupture (MPa)	Thickness Swelling Rate of Water Absorption (%)
1.51 ± 0.15	1.63 ± 0.11	30.98 ± 1.47	0.5 ± 0.1

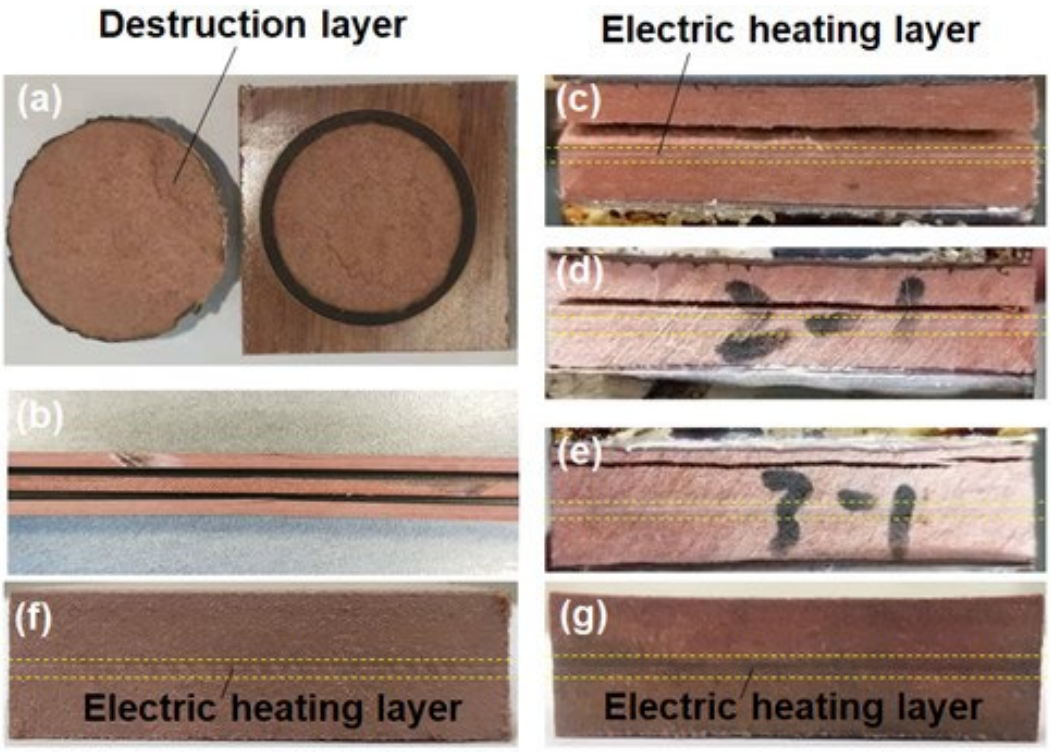

Fig. 15. The physical and mechanical performance tests on the electric heating floor. The specimens a) for the surface bonding strength test, b) for the modulus of rupture test, c-e) for the internal bonding strength test, f) before the thickness swelling rate of water absorption test, and g) after the thickness swelling rate of water absorption test.

CONCLUSIONS

1. The presented large-format manufacture process further effectively improved the production efficiency of the electric heating floor, by which the carbon fiber paper electric heating layer with good permeability can be penetrated by melamine resin to strengthen the lap structure among the carbon fibers. The floor exhibited good bonding performance even though the carbon fiber paper was combined in two-layers of fiberboard substrates.
2. After the single electric heating floor was energized for 12 h under the voltage of 220 V, the DRR was as low as approximately 1.2%. The surface temperature rise reached about 20 °C after energized for 1 h. The floor also had a uniform temperature distribution on its surface.
3. The assembled electric heating floors also exhibited uniform distribution of surface temperature and good power stability in the long-term running process. Moreover, there was small temperature difference as low as approximately 2 °C at the height range from 0.6 m to 1.8 m above the floors. The surface temperature rise of the floors could reach about 25 °C after 105 min. After the assembly, all the electric heating floors displayed similar temperature rise performance and uniformity, which indicated that the large-format process is feasible.
4. The electric heating layer in the presented electric heating floor is closer to the heating space, compared to that in the floor heating system with the wood floor covering on electric heating system, which helps to improve the heat transfer speed and reduce heat loss.

ACKNOWLEDGMENTS

The authors are grateful for the support of the Guangxi Innovation-Driven Development Special Fund Project of China (Guike AA17204087-18) and the Scientific Research and Technology Development Project of Nanning of China (20175030-2). The authors are also grateful to Guangxi Bojing Floor Co., Ltd. (Nanning, China) for providing relevant help.

REFERENCES CITED

Boahen, S., Anka, S. K., Lee, K. H., and Choi, J. M. (2021). "Performance characteristics of a cascade multi-functional heat pump in the winter season," *Energy and Buildings* 253, article no. 111511. DOI: 10.1016/j.enbuild.2021.111511

Di, W., Zhang, G., Xu, J., Peng, Y., Wang, X., and Xie, Z. (2003). "Positive-temperature-coefficient/negative-temperature-coefficient effect of low-density polyethylene filled with a mixture of carbon black and carbon fiber," *Journal of Polymer Science Part B Polymer Physics* 41(23), 3094-3101. DOI: 10.1002/polb.10594

GB/T 18102 (2020). "Laminate floor coverings," Standards press of china, Beijing, China.

Gong, X., Liu, L., Liu, Y., and Leng, J. (2016). "An electrical-heating and self-sensing shape memory polymer composite incorporated with carbon fiber felt," *Smart Materials and Structures* 25(3), 035036. DOI: 10.1088/0964-1726/25/3/035036

Pradere, C., Batsale, J., Goyheneche, J., Pailler, R., and Dilhaire, S. (2009). "Thermal properties of carbon fibers at very high temperature," *Carbon 47*(3), 737-743. DOI: 10.1016/j.carbon.2008.11.015

Sarbu, I., and Sebarchievici, C. (2014). "A study of the performances of low-temperature heating systems," *Energy Efficiency* 8(3), 609-627.DOI: 10.1007/s12053-014-9312-4

Seo, J., Jeon, J., Lee, J.-H., and Kim, S. (2011). "Thermal performance analysis according to wood flooring structure for energy conservation in radiant floor heating systems," *Energy and Buildings* 43(8), 2039-2042. DOI: 10.1016/j.enbuild.2011.04.019

Song, J., Hu, H., Zhang, M., Huang, B., and Yuan, Z. (2017). "Thermal aging properties and electric heating behaviors of carbon fiber paper-based electric heating wood floors," *BioResources* 12(4), 9466-9475. DOI: 10.15376/biores.12.4.9466-9475

Song, J., Yuan, Q., Liu, X., Wang, D., Fu, F., and Yang, Y. (2015). "Combination of nitrogen plasma modification and waterborne polyurethane treatment of carbon fiber paper used for electric heating of wood floors," *BioResources* 10(3), 5820-5829. DOI: 10.15376/biores.10.3.5820-5829

Wang, J., Lou, T., Wang, T., Cao, W., and Geng, H. (2021). "Flexible electrothermal laminate films based on tannic acid-modified carbon nanotube/thermoplastic polyurethane composite," *Industrial & Engineering Chemistry Research* 60(21), 7844-7852. DOI: 10.1021/acs.iecr.1c00964

Yang, S., Su, C., Song, L., and Yuan, Q. (2017). "Composite process and electrothermal properties of a new-type electric heating plywood made with melamine resin adhesive film," *BioResources* 12(4), 8953-8969. DOI: 10.15376/biores.12.4.8953-8969

Yi, X., Zhao, D., Ou, R., Ma, J., Chen, Y., and Wang, Q. (2017). "A comparative study of the performance of wood-plastic composites and typical substrates as heating floor," *BioResources* 12(2), 2565-2578. DOI: 10.15376/biores.12.2.2565-2578

Yuan, Q. P., and Fu, F. (2014). "Application of carbon fiber paper in integrated wooden electric heating composite," *BioResources* 9(3), 5662-5675. DOI: 10.15376/biores.9.3.5662-5675

Zhao, H., Wu, Z., Wang, S., Zheng, J., and Che, G. (2011). "Concrete pavement deicing with carbon fiber heating wires," *Cold Regions Science and Technology* 65(3), 413-420. DOI: 10.1016/j.coldregions.2010.10.010

Article submitted: December 18, 2021; Peer review completed: March 12, 2022; Revised version received and accepted: March 27, 2022; Published: May 13, 2022.
DOI: 10.15376/biores.17.3.4069-4085